Linking Nonlinear Tactile Elements by Cell-Bridge System

Takayuki Hoshi*and Hiroyuki Shinoda*

The goal of our research is a practical robot skin that covers a large area of a robot surface, senses various touch feelings, and is soft and stretchable. We are developing a tactile sensor array by linking the sensor elements proposed in the previous sensor symposium. The sensor element acquires not only a contact force but also a contact area within its large (several cm sq.) sensing area. The structure of the sensor element is very simple; two layers of compressible insulators (urethane foam) which are sandwiched between three layers of stretchable conductive sheets (conductive fabric). The structure enables us to obtain the two parameters from the capacitances between the conductive layers. In linking the sensor elements, we apply the "cell-bridge-based networking system" in which no long wires are included. CMOS LSI sensor/communication chips are arranged at the boundaries of the sensor elements, and the chips measure the capacitances between the conductive layers and send signals through the same conductive layers. In the array structure, the contact position can be estimated with finer resolution than the size of the sensor element by calculating the spatial centroid from the measured contact forces.

Keywords : Tactile sensor, Robot skin, Haptic interface, Contact area, Nonlinear elasticity, Cell bridge

1. Introduction

Humanoids [1][2] and pet robots [3][4] need touch feelings in order to handle unpredictable events and communicate with humans safely. To realize that, robot skins which give tactile sensation to such robots are demanded in robotics [5]. Such a robot skin should (i) sense rich tactile information sensitively, (ii) cover a several-m^2 large area such as a whole surface of a robot, and (iii) be soft and stretchable to contact humans or objects safely and fit a robot surface. The third property, softness, is also important to detect touch feelings effectively.

For that purpose, various kinds of robot skins are reported until now [6]-[11]. Almost all of them are arrays of sensor elements that measure only one parameter, averages of pressure distributions within their sensing areas, and in consequence, the elements have to be arrayed in high density in order to obtain rich tactile information. In that situation, a large number of sensor elements and wirings are troublesome and some breakthroughs are needed to overcome the problem.

We have proposed a new tactile sensor element that obtains rich tactile information in another approach [12]. The sensor element measures two parameters, not only the summation of the pressure distribution (the contact force) but also the degree of its extent (the contact area), within its several-cm-sq. sensing area. Owing to the additional sensing parameter, the contact area, a robot skin which detects minute shape features is easily realized by arraying the elements in low density. This proposition is based on the characteristics of the human tactile sensation. While Two Point Discrimination Thresholds (TPDT) of humans are as large as 2-5 cm except on faces and hands [13], humans can discriminate sharpness of objects sensitively even on such large TPDT parts. From these facts, we suppose that sharpness is one of key components to produce general human tactile sensation [14], and that sensitivity to the sharpness is a high priority for a human-like sensor skin. Because the sensing theory is based on the nonlinear elasticity of the material, the sensor element is named the "nonlinear tactile element".

In this paper, we introduce how the sensor elements are linked to make up a robot skin. The "cell-bridge system" [15] is applied to link them without long wires. The resulting robot skin can estimate the contact position with finer resolution than the size of the sensor element owing to the array structure.

The rest of this paper is organized as follows. Firstly, Section 2 describes the proposed "nonlinear tactile element". After that, we explain the "cell-bridge system" and the structure of the robot skin in Section 3. In Section 4, the estimation of the contact position is demonstrated. Finally, we conclude this paper in Section 5.

2. Nonlinear tactile element [12]

2.1 Structure   The structure of our sensor element is very simple. In Fig.1, we show schematically the cross-section of the sensor element prototype. The sensor element consists of two insulator layers; the upper and lower layers are soft (15 kg/m^3) and hard (60 kg/m^3) urethane foam, respectively, and each layer is 2 mm in thickness. There are three pieces of stretchable conductive fabric on the soft layer, between the soft and hard, and under the hard. Each piece has an area of 30×30 mm^2. The side length of the conductive fabric piece is comparable to the TPDT on human forearms. The insulator layers and the conductive pieces adhere to each other by soft double-faced tape, and two capacitors are formed in the layers. Supposing a surface of a robot body hard, we attach the bottom of the sensor element prototype to an acrylic base in the experiments (Section 2.3).

2.2 Sensing theory   We suppose an uniform pressure distribution $\sigma(x, y)$ [Pa] is vertically loaded to the surface of the sensor element in a contact field S, that is,

$$\sigma(x,y) \equiv \begin{cases} F/S & \text{if } (x, y) \in \text{S} \\ 0 & \text{if } (x, y) \notin \text{S} \end{cases} \quad \cdots\cdots\cdots (1)$$

* Department of Information Physics and Computing, Graduate School of Information Physics and Technology, the University of Tokyo, 7-3-1 Hongo, Bunkyo-ku, Tokyo, Japan 113-8656
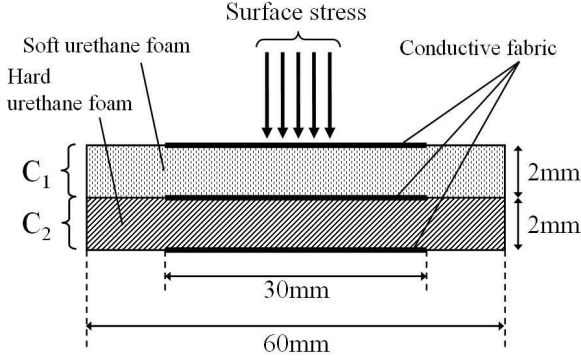
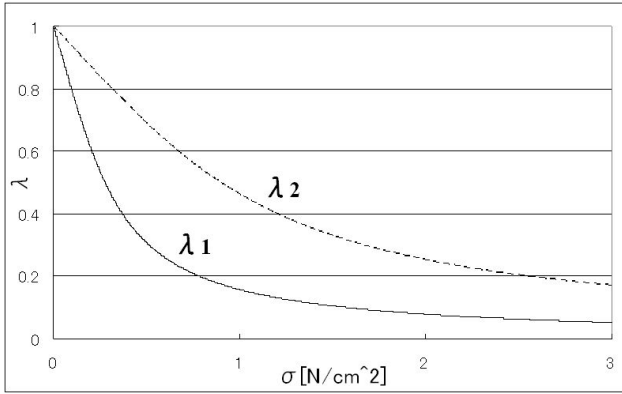Figure 1. Cross-section of prototype of one tactile sensor element. [12]

Figure 2. Relationship between surface stress σ and extension ratio λ_n. The soft layer λ_1 is more easily compressed than the hard layer λ_2. [12]

where F [N] is the total intensity of the contact force and S [m^2] is the area of S. Now we take note of the area of S, not the shape, so we suppose that S is circular for simplicity.

We also assume as follows. First, the nonlinear elasticity of the insulator layers is the entropy elasticity [16] expressed as

$$\sigma = \frac{E_n}{3}\left(\frac{1}{\lambda_n} - \lambda_n^2\right) \quad (n = 1, 2) \quad \cdots\cdots\cdots (2)$$

$$\lambda_n \equiv 1 - \frac{\Delta d_n}{d_n - d_{n0}} \quad \cdots\cdots\cdots\cdots (3)$$

where n is the layer identification; $n=1$ means the upper soft layer and 2 the lower hard layer. E_n [Pa], d_n [m], d_{n0} [m] and λ_n are the elasticity modulus, the initial thickness, the saturated thickness and the extension ratio of the layer n, respectively. E_1 is about 4.8 kPa and E_2 is 15 kPa by actual measurement. The following expression of λ_n (Fig.2) is obtained by solving Eq.(2),

$$\lambda_n = \sqrt[3]{\frac{1}{2} + \sqrt{\frac{1}{4} + \left(\frac{\sigma}{E_n}\right)^3}} + \sqrt[3]{\frac{1}{2} - \sqrt{\frac{1}{4} + \left(\frac{\sigma}{E_n}\right)^3}} . \quad \cdots\cdots (4)$$

Second, the conductive pieces have negligible tensions and the Poisson's ratios of the insulator layers are zero, which means that a displacement distribution $\Delta d_n(x, y)$ [m] is determined simply by the local value of $\sigma(x, y)$.
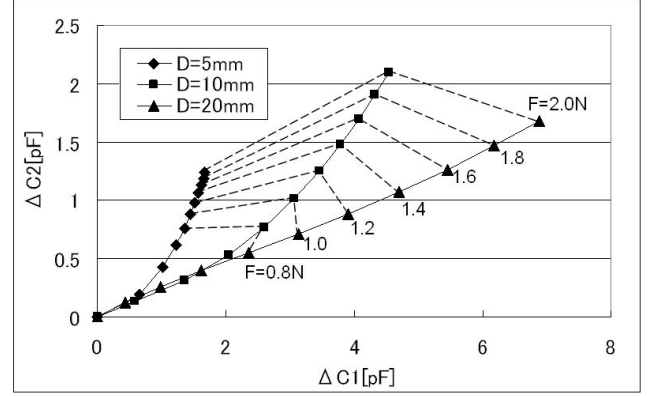

Figure 3. Simulation results. Calculated (ΔC_1, ΔC_2)s for various (F, S)s. D is a parameter defined as $D \equiv 2\sqrt{S/\pi}$ to represent a diameter of S for a circular object. [12]

We measure electric capacitances C_n [F] between the conductive pieces to detect $\Delta d_n(x, y)$. Ignoring fringing fields, the capacitance is formulated as

$$C_n = \iint_{Element} \frac{\varepsilon_n}{d_n - \Delta d_n(x, y)} \mathrm{d}x\mathrm{d}y \quad \cdots\cdots\cdots\cdots (5)$$

where ε_n [F/m] is the dielectric constant of the layer n. If we can make the second assumption mentioned above, (C_1, C_2) is uniquely determined by (F, S). Then the key question is whether the inverse mapping from (C_1, C_2) to (F, S) is possible or not for the layers 1 and 2 having different hardness.

Figure 3 shows the results of a numerical simulation for the elasticity moduli $E_1 = 4.8$ kPa and $E_2 = 15$ kPa. It shows that the plot of (ΔC_1, ΔC_2)s for various (F, S)s spans a two dimensional space, where (ΔC_1, ΔC_2) are the capacitance differences by the applied force, and D is a parameter defined as

$$D \equiv 2\sqrt{S/\pi} \quad \cdots\cdots\cdots\cdots\cdots\cdots\cdots\cdots (6)$$

to represent the diameter of S for a circular object. It implies that we can determine (F, S) uniquely from (ΔC_1, ΔC_2) when F is larger than a threshold, now around 1.0 N.

Note that the nonlinear elasticity of the insulator layers plays a key role in the sensing theory explained here. In the case of linear elastic insulator layers, i.e. $\sigma << E_n$, it is impossible to estimate S from (C_1, C_2). λ_n of the linear elastic insulator is calculated by approximating Eq.(4) as

$$\lambda_n \cong 1 - \sigma/E_n . \quad \cdots\cdots\cdots\cdots\cdots\cdots\cdots (7)$$

Then Eq.(5) can be approximated as

$$C_n \cong C_{n0} + \varepsilon_n F/d_n E_n \quad \cdots\cdots\cdots\cdots\cdots\cdots (8)$$

where C_{n0} is the initial capacitance of the layer n. Equation (8) means that neither C_1 nor C_2 contains the parameter S.
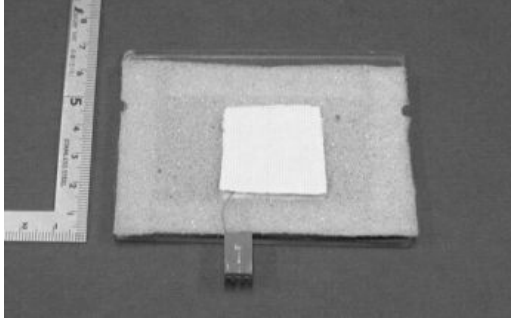
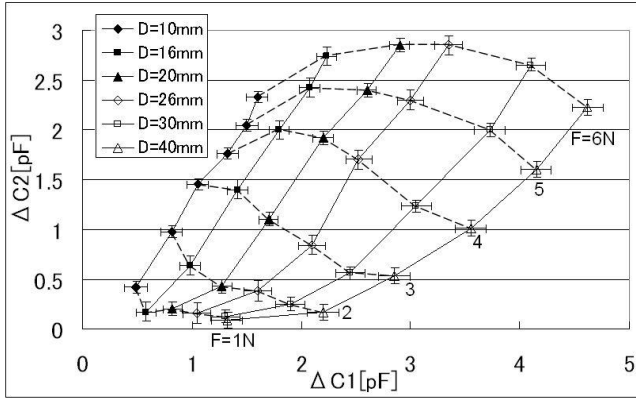Figure 4. Photograph of sensor element prototype. [12]

Figure 5. Experimental results of five trials. Averaged trajectories of $(\Delta C_1, \Delta C_2)$s for various (F, S)s with error bars representing maximal deviations. [12]

2.3 Experiments and results

We conducted experiments to examine the feasibility of the proposed sensing method. We measured C_n of the sensor element prototype (Fig.4) by a self oscillation method; we generated a RC oscillation including the sensor element as the capacitor, and counted pulses par 2 ms by a 16-bit counter. A PC imported data via a digital I/O, and achieved about 40 Hz effective sampling rate. We used six acrylic stimulators with diameters D = 10, 16, 20, 26, 30, and 40 mm. Each stimulator was vertically pressed at the center of the sensor element. It was operated quasi-statically by a mechanical z-stage, with measuring the pressing force F by a weighting machine.

Figure 5 shows how (F, S)s are represented in the $(\Delta C_1, \Delta C_2)$ space. It is confirmed that the plot of $(\Delta C_1, \Delta C_2)$s spans a two dimensional space sufficiently. The reason of the quantitative difference from the simulation result (Fig.3) is considered to be the tension of the actual conductive fabric.

3. Linking sensor elements

3.1 Cell-bridge system

The "cell-bridge system" is a novel signal transmission system which is constructed by "cells" and "bridges" [15]. The bridge is a communication chip that can transmit and receive electric signals. The cell is a two-dimensional medium through which the bridges exchange signals each other. Many kinds of such materials as conductive rubber or fabric are available for it. By connecting sensor elements to the cells, we can realize a high-density sensor network.

Furthermore, the cell-bridge system is effective when the cells are given additional functions of sensor or actuator. For example,
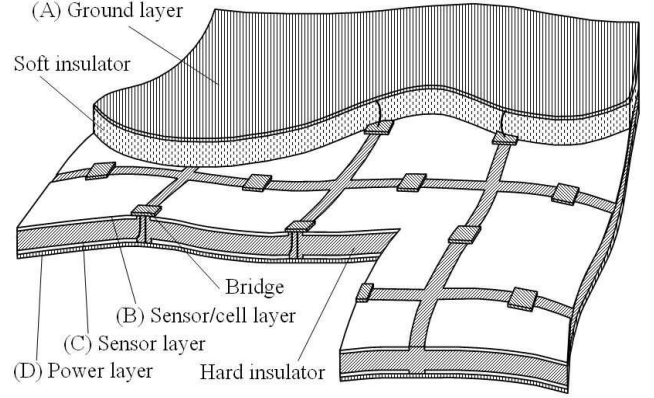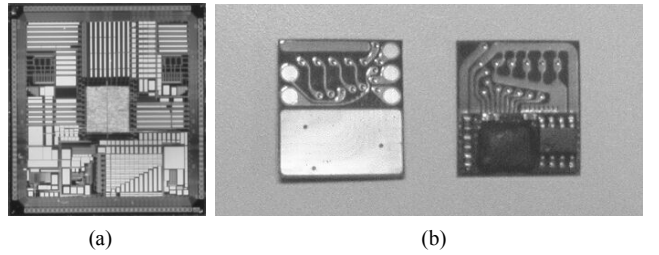

Figure 6. Illustration of proposed robot skin.

(a)   (b)

Figure 7. (a) Closeup top view of prototype of CMOS LSI (5×5 mm^2). (b) LSI packaged on flexible substrate (16×18 mm^2, opened).

the cells are given the function of electrostatic speaker in [17]. In this paper, we apply this system to a robot skin.

3.2 Structure of robot skin

Figure 6 shows the structure of the proposed robot skin. There are two compressible insulator layers which have different stiffness. Besides, there are four stretchable conductive layers; the conductive layers A, B, C, and D are the ground layer, the sensor/cell layer, the other sensor layer, and the power layer, respectively. The conductive layers A and B sandwich the soft insulator layer forming the capacitor named C_1, and B and C sandwich the hard insulator layer forming C_2. This pair of the capacitors is one tactile sensor element. The conductive layers C and D are isolated by the thin stretchable insulator layer. The bridge is mounted in the structure and connected to the conductive layers locally by short wires. It is supplied power from the layers A and D (the ground and power layers). These two layers also function as electrostatic shields. It measures the capacitances C_n [F] (n = 1, 2) and sends measured data to the host computer through the conductive layer B (the cell layer) by multi-hoping method. The structure described here can maintain the softness of the robot skin because it contains no long wires.

3.3 Prototype

At the present stage, we have completed fabrication of the first prototype of CMOS LSI based on 0.35 μm rules for the bridges (Fig.7 a). While the size of the LSI is 5×5 mm^2, the total area of the analog-digital mixed circuits is within 1.5 mm^2. The operating frequency of the LSI is 50 MHz. Each bridge measures C_n by an 8-bit A/D converter and it has a function to transmit the data to the neighboring chip. We packaged the LSI on a compact (16×18 mm^2) flexible substrate (Fig.7 b) that is folded in half (16×9 mm^2). Although this first prototype needs an additional front-end circuit IC (5×6 mm^2), the next version will not need it and can be packaged in a substrate that is almost half in size of the present one.
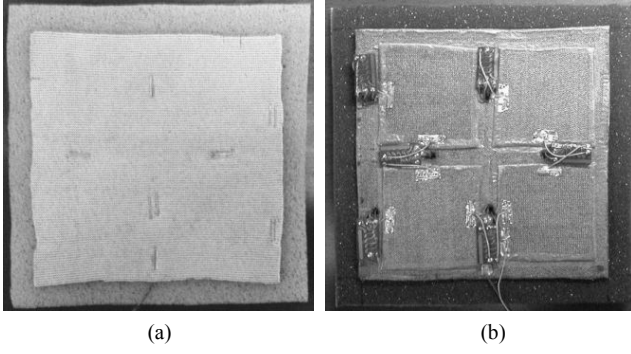
Figure 8. Developed 2×2 tactile sensor array. Each sensor element is 40×40 mm². (a) and (b) are top and bottom views of the test model.
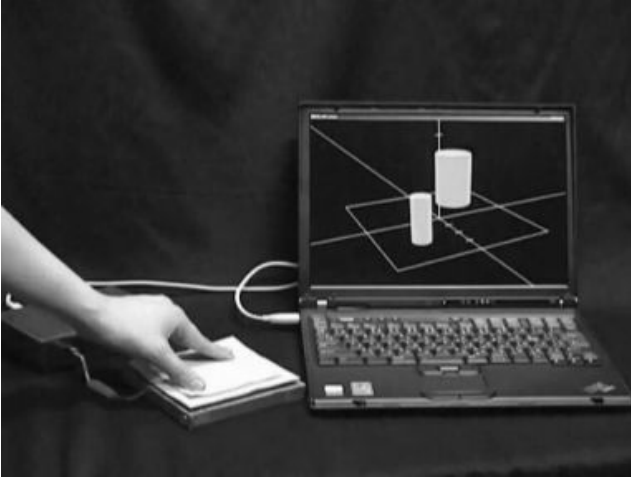

Figure 9. Demonstration I. One element (near side) is pressed by the thumb, and the other (far side) by the first and second fingers. F and S (the height and the area of the base of the column) are estimated.

We developed a test model of the robot skin (Fig.8) using the first prototype of the LSI. For the simplicity of the protocol, there are additional layers for signal transmission (i.e. the layer B in Fig.6 is only used as the sensor layer). The test model is a 2×2 array and the size of each element is 40×40 mm². We verified that the bridges measured the capacitances of the sensor elements and the data were transmitted to the host computer successfully. In Fig.9, we demonstrate that F (the height of the column) and S (the area of the base of the column) are estimated using the transmitted data from the bridges.

4. Estimating contact position

4.1 Basic theory The proposed sensor element has no sensitivity to the contact position within its sensing area because C_n is a spatial integrated value (see Eq.(5)). In consequence, the localization ability of the robot skin seems to be limited by the size of the sensor element.

Generally, in fact, it is possible to estimate the contact position from the output data of the discrete sensor elements if their receptive areas overlap each other. For example, we suppose two adjacent sensors of which the sensitivity distributions f_i ($i = 1, 2$) are the Gaussian distributions (Fig.10 a) expressed as

$$f_i(x) = \exp\left\{-(x - x_i)^2 / s^2\right\} \quad \cdots\cdots\cdots\cdots\cdots\cdots\cdots (9)$$
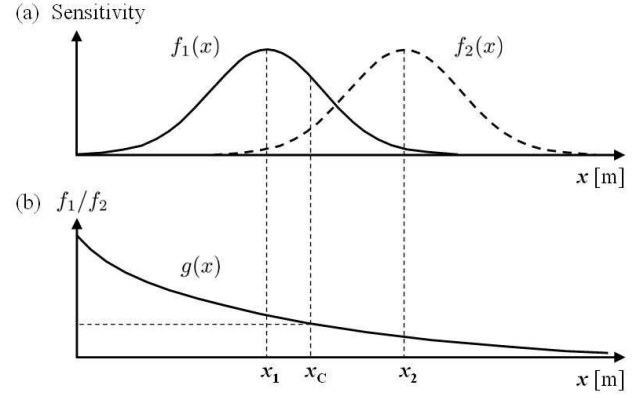

Figure 10. (a) Supposed Gaussian sensitivity distribution, f_1 and f_2. (b) Ratio of f_1 to f_2. The contact position x_C can be estimated from the ratio of the measured data.

where i is the element identification. x_i [m] and s [m] are the means and the standard variation, respectively. When a force F is applied to the elements at x_C [m], their outputs are expressed as $F \times f_i(x_C)$. So the ratio of the outputs are calculated as

$$g(x_C) \equiv \frac{F \times f_1(x_C)}{F \times f_2(x_C)} = \alpha \exp(-\beta\, x_C), \quad\cdots\cdots\cdots\cdots (10)$$

$$\alpha \equiv \exp\left\{(x_2^2 - x_1^2)/s^2\right\}, \quad\cdots\cdots\cdots\cdots\cdots\cdots\cdots\cdots (11)$$

$$\beta \equiv 2(x_2 - x_1)/s^2 . \quad\cdots\cdots\cdots\cdots\cdots\cdots\cdots\cdots\cdots (12)$$

From Eq.(10), we can derive the contact position x_C (Fig.10 b) as

$$x_C = g^{-1}(f_1/f_2). \quad\cdots\cdots\cdots\cdots\cdots\cdots\cdots\cdots\cdots (13)$$

While the theory explained here is based on the Gaussian sensitivity distribution, its basics also hold true with other types of sensitivity distributions.

4.2 Experiments and results We conducted experiments to examine the possibility of the estimation of the contact position. Figure 11 shows ΔC_1 and ΔC_2 of the two adjacent elements A and B when the pressing position moves along their center line. It turns out that both sensor elements respond at the same time when the stimulator contacts both of them. This fact indicate that it is possible to estimate the contact position in our robot skin when the stimulator moves beyond the boundaries between the sensor elements, although it is still impossible to estimate the contact position when the stimulator moves within one sensor element.

The estimation of the contact position is demonstrated in Fig.12. In this demo, we calculate simply the spatial centroid from the measured contact forces and consider it as the contact position.

5. Conclusion

In this paper, we constructed the robot skin by combining the two technologies; the nonlinear tactile element and the cell-bridge system. We also proposed and demonstrated that the localization ability was enhanced by calculating the spatial centroid from the measured contact forces.

Figure 11. Experimental results. ΔC_1 and ΔC_2 of the two adjacent sensor elements. The stimulator ($D = 10$ mm) was vertically pressed at $F = 3$ N. A and B respond at the same time when both of them are pressed.

Figure 12. Demonstration II. The two adjacent sensor elements are pressed by the spherical stimulator. The height and the standard variation of the Gaussian distribution means F and $D/4$, respectively. In addition to the two parameters, the contact position is also estimated.

Acknowledgement

References

(1) Y. Sakagami, R.Watanabe, C. Aoyama, S. Matsunaga, N. Higaki, and K. Fujimura, "The Intelligent ASIMO: System Overview and Integration," Proc. the 2002 IEEE/RSJ International Conference on Intelligent Robots and Systems (IROS 2002), vol. 3, pp. 2478-2483 (2002)

(2) K. Kaneko, F. Kanehiro, S. Kajita, H. Hirukawa, T. Kawasaki, M. Hirata, K. Akachi, and T. Isozumi, "Humanoid Robot HRP-2," Proc. the IEEE 2004 International Conference on Robotics and Automation (ICRA 2004), vol. 2, pp. 1083-1090 (2004)

(3) T. Shibata, K. Wada, and K. Tanie, "Tabulation and Analysis of Questionnaire Results of Subjective Evaluation of Seal Robot in Japan, U.K., Sweden and Italy," Proc. the IEEE 2004 International Conference on Robotics and Automation (ICRA 2004), vol. 2, pp. 1387-1392 (2004)

(4) M. Fujita, "AIBO: Toward the Era of Digital Creatures," The International Journal of Robotics Research, vol. 20, no. 10, pp. 781-794 (2001)

(5) M. H. Lee, and H. R. Nicholls : "Tactile Sensing for Mechatronics - A State of the Art Survey", Mechatronics, vol. 9, pp. 1-31 (1999)

(6) E. S. Kolesar and C. S. Dyson, "Object Imaging with a Piezoelectric Robotic Tactile Sensor," IEEE Journal of Microelectromechanical Systems, vol. 4, pp. 87-96 (1995)

(7) Y. Hoshino, M. Inaba, and H. Inoue, "Model and Processing of Whole-Body Tactile Sensor Suit for Human-Robot Contact Interaction", Proc. the 1998 IEEE International Conference on Robotics & Automation (ICRA '98), pp. 2281-2286 (1998)

(8) R. Kageyama, S. Kagami, M. Inaba, and H. Inoue, "Development of Soft and Distributed Tactile Sensors and the Application to a Humanoid Robot", Proc. the IEEE International Conference on Systems, Man, and Cybernetics, vol. 2, pp. 981-986 (1999)

(9) F. Castelli, "An Integrated Tactile-Thermal Robot Sensor with Capacitive Tactile Array," IEEE Transactions on Industry Applications, vol. 38, no. 1, pp. 85-90 (2002)

(10) O. Kerpa, K. Weiss, and H. Worn, "Development of a Flexible Tactile Sensor System for a Humanoid Robot", Proc. the 2003 IEEE/RSJ International Conference on Intelligent Robots and Systems (IROS 2003), vol. 1, pp. 1-6 (2003)

(11) M. Shimojo, A. Namiki, M. Ishikawa, R. Makino, and K. Mabuchi, "A Tactile Sensor Sheet Using Pressure Conductive Rubber with Electrical-Wires Stitched Method," IEEE Sensors Journal, vol. 4, no. 589-596 (2004)

(12) T. Hoshi and H. Shinoda, "A Tactile Element Based on Nonlinear Elasticity to Sense Contact Area," Proc. 22nd Sensor Symposium, pp.375-379 (2005)

(13) S. Weinstein, "Intensive and Extensive Aspects of Tactile Sensitivity as a Function of Body Part, Sex, and Laterality," The Skin Senses, C. C. Thomas, pp. 195-222 (1968)

(14) Y. Makino, N. Asamura, and H. Shinoda, "Multi Primitive Tactile Display Based on Suction Pressure Control", Proc. IEEE 12th Symposium on Haptic Interfaces for Virtual Environment and Teleoperator Systems (Haptic Symposium 2004), pp. 90-96 (2004)

(15) A. Okada, Y. Makino, and H. Shinoda, "Cell Bridge: A Signal Transmission Element for Constructing High Density Sensor Networks," Proc. 2nd International Workshop on Networked Sensing Systems (INSS 2005), pp. 180-185 (2005)

(16) G. R. Strobl, "The Physics of Polymers: Concepts for Understanding Their Structures and Behavior", Chap. 7, Springer (1997)

(17) A. Okada, Y. Makino, and H. Shinoda, "Cell-Bridge-Based Connection Method of High Density Sensor Elements," Proc. 22nd Sensor Symposium, pp. 425-428 (2005)
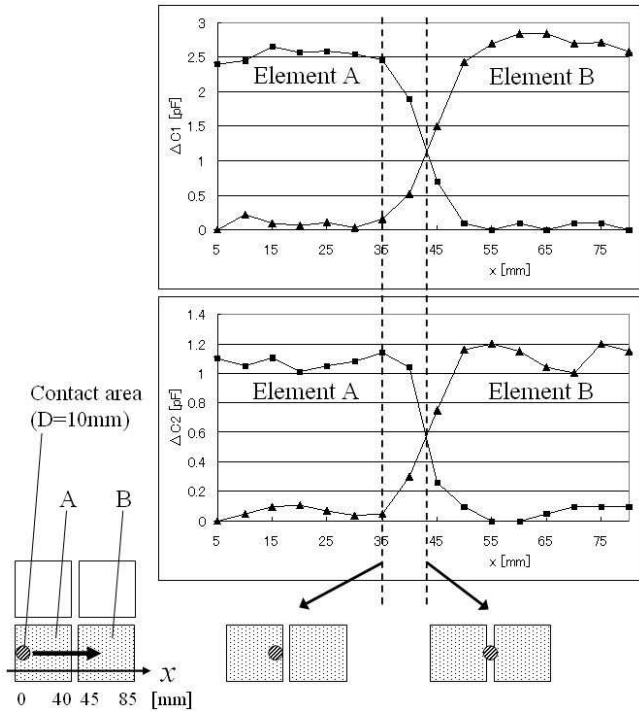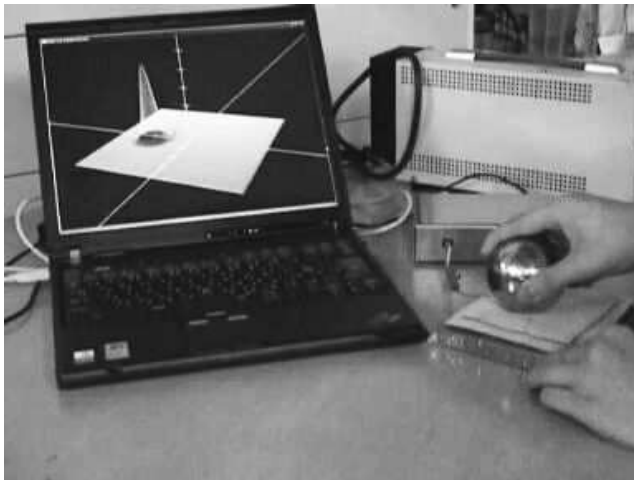
278